World Journal of Advanced Engineering Technology and Sciences
eISSN: 2582-8266
Cross Ref DOI: 10.30574/wjaets
Journal homepage: https://wjaets.com/

(REVIEW ARTICLE)

Check for updates

Effect of rail cant on stress distribution

Tiago Tepedino [1, 2], Marcelo Leite Ribeiro [2] and Gustavo Tressia [3, *]

[1] *Loram of Brazil, Curitiba, Brazil.*
[2] *Aeronautical Engineering Department, São Carlos School of Engineering, University of São Paulo, São Carlos, Brazil.*
[3] *Vale Institute of Technology, Ouro Preto, Brazil.*

World Journal of Advanced Engineering Technology and Sciences, 2023, 09(01), 372–386

Publication history: Received on 09 May 2023; revised on 18 June 2023; accepted on 21 June 2023

Article DOI: https://doi.org/10.30574/wjaets.2023.9.1.0184

Abstract

The rail cant is an important geometry parameter and is commonly monitored to ensure railway safety and comfort conditions. Understanding the influence of cant variation on the performance of railway components is extremely important to define the tolerance limits of the track and adequacy of maintenance plans. There are numerous rail cant patterns on railways, 1:40, 1:30, 1:20. However, the optimal rail cant to reduce the stress and wear of rail head not been extensively studied. This work performs an analysis of the effect of the rail cant on the rail head stress distribution. To investigate stress and strain in rail head, a Finite Element Model with Ansys software was used. For the analysis was considered a 136RE rail, axle load of 32 ton and AAR-1B wheel profile. The rail cant was varied in 0, 1:20 and 1:40. The results show that the stress in rail and wheel increases with the rail cant. The maximum stress occurred in the condition with rail cant of 1:20. The variation of cant from 0 to 1:20 results in a decrease of approximately 9% in maximum stress, ranging from 947 MPa to 867 MPa. The wheel/rail contact in cant zero condition occurred close to the transition of the wheel tread and the beginning of flange root, resulting in a dynamic instability in the wheelset. In addition to higher contact stress, increases the propensity for the hutting phenomenon, which can accelerate rail and wheel wear

Keywords: Rail cant; Rail; Wheel railway; FEM

1. Introduction

One of the variables for the development of the optimized rail profile is the cant (Shevtsov, 2008). The rail cant is the angle resulting from the rotation around its longitudinal axis towards to the inner direction of the rail (Zakeri et al 2011). This approach is currently used by all the main railways. Typically, the rail is tilted inwards toward the gauge, a cant between 1/20 to 1/40, helping to maintain the vertical contact point and centered on the railhead, since the railway wheel is conical (Sadeghi et al., 2009). One important consequence of the cant variation is the increase of the propensity to derailment due to the gauge opening and/or buckling of the rail. Cant variations of the rails diverging from the parameters specified, can lead to a more accelerated degradation of the components of the permanent way and among other losses to the railways (Sadeghi et al., 2009). Arema suggested the rail cant 1/40, however, this value is not a consensus, in Iranian railways, most European railway, in Russian railway and Canadian railways the cant is 1/20, in German railway the rail cant is 1/40 and in Union Pacific railway the cant is 1/30 (Zakeri et al 2011).

Some studies show the importance of the cant of the rails in the railways, both in relation to changes of the wheel-rail contact and in relation to the dynamic interaction (Ovchinnikov et al., 2021; Sadeghi et al., 2009; Shevtsov, 2008; Wang et al., 2013). However, none of them deal with cant values that railway maintenance should have as limits, that is, the studies do not establish how much the cant can vary and what would be the maintenance limits of this parameter.

* Corresponding author: G. Tressia

Wang et al (2019) studied the influence of rail cant on the wear of high rail side of a small radius curve in urban rail lines. For a condition, with a small curve radius, of 375 m, a reduction in wheel wear was found when using rail cant of 1/40. Li et al (2021), developed a numerical prediction model for the wheel-rail wear and showed that on curved track the rail cant of 1/30 is recommended to reduce wear of the system. Wang et al (2013) analyzed the rail cant influence on the basis of the wheel-rail spatial contact geometry algorithm and showed that with the increase of rail cant from 1/40 to 1/20 results in increase of the corresponding rolling radius difference, contact angle parameter, equivalent conicity and equivalent contact angle parameter, which means the self-centring capacity of wheelset is enhanced and the wheel-rail relationship is improved. Additionally, with rail cant of 1/20 the probability of the wheel flange contact is reduced and consequently the wear of wheel and railhead tread is minimized. Finally, in curve track, increase the rail cant from 1/40 to 1/20 reduce the interaction of wheel and rail, increase the contact area between wheel and rail, promoting a lower contact stress and contact fatigue defects are reduced.

The results of the influence of rail cant are dependent on axle load, speed, track condition and other parameters that vary from railroad to railroad, so it is very difficult to find a single value that results in lower wear and better dynamic conditions. Therefore, the development of models, approaches and analyzes is extremely important for evaluation and selection of the best Cant, as well as its permissible limits of variation.

This study aims to analyze the contact pressures, the stresses, as a result of the cant variations in the rail of: 0, 1/20 and 1/40, compare the results obtained in the wheel/rail contact, analyze the maximum stresses occurring both on the wheel and rail using the Von Mises criterion.

2. Methodology

2.1. Wheel-rail model

The model used was a railway track segment containing 32 timber sleepers spaced out totaling 550 mm. 32 mounting plates for type E-2009 clip were placed and overlaid on the sleepers. The modeled rail was the 136RE and the AAR-1B wheel profile and a 1600 mm gauge was maintained for all cants. In order to impose the greatest efforts for the rail, four wheels were placed in the model. A pair of wheels represented the bogie of a wagon and the other pair the bogie of a wagon next to it. The distance between the top plates of the two bogies was 4127 mm, while the measure between wheelsets in the same bogie was 1778 mm. Also, the effect of gravity was considered.

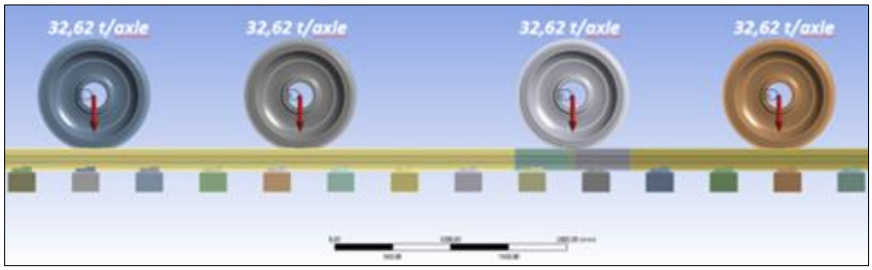

Figure 1 Side view of the model

For the simulations, ANSYS software and Envision was used.

In order to represent the normal force that the clip exerts on rail a spring element was created in the exact location where the clip touches the rail. The modeled stiffness for this spring was 1700 N/mm and a pre-load of 12263 N was applied representing a clip in its new state.

In order to represent the stiffness that the ballast exerts on the sleeper, an elastic support condition was established at the base of the sleeper with 0.05 N/mm^3. In addition, a displacement condition was established on the external faces of the sleepers with restriction of the z component and on the lateral faces of the sleepers with restriction of displacements in the direction of the x component

The type of contact used between the plates and the sleepers was *bonded*, in this type of contact there is no creeping or separation between the faces or edges and this contact allows for a linear solution. Now, the contact between the rail and the mounting plates was of the frictional type with a friction coefficient of 0.5, in this type of contact creeping friction and separation of the faces or edges is allowed and a non-linear solution is calculated. This same type of contact was

established between the rolling surfaces of the wheels and the rail surface, however the coefficient of friction for these contacts was 0.4 and a symmetrical behavior was adopted in the center line.

With the same contour conditions, however, varying the profile of the rail and maintaining the profile of the wheel, 5 types of profiles were simulated. The first model represents the contact of a new rail profile. The second (Profile A) represents the contact of a tangent profile built by adjusting a point cloud through a spline with a tolerance of 0.001 mm. The third (Profile B) represents a profile constructed by segments of arcs with radius and initial and final coordinates of the well-defined segments. The fourth (Profile C) represents a tangent profile that favors the central contact for cant 1/40, while the fifth (Profile D) represents a profile that favors a field contact for cant 1/40, both were constructed by segments of arches with radius and coordinates, also, well defined.

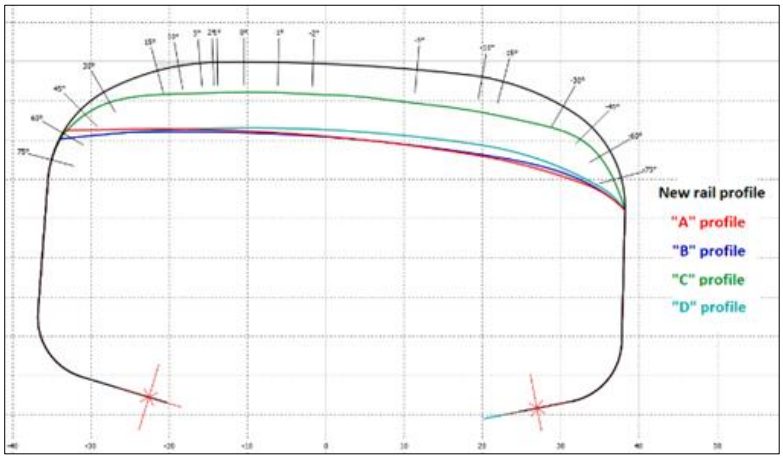

Figure 2 View of the analyzed profiles

With the intention of capturing with better quality the effects of the wheel-rail contact the technique of sub-modeling was used in a segment of the track simulated under a wheel. Through this technique it was possible, computationally, to define in the contact region a grid of hexagonal quadratic elements with a size of 0.75 mm. In the sub-model, they had about 800 thousand nodes and 300 thousand elements in the finite element mesh.

The material used has elasto-plastic behavior and the multi-linear kinematic strain hardening model was used. The construction of this model was possible by separating the elastic and plastic part of the tensile test data from a rail and wheel material with a hardness of 400HB.

3. Result

For the profile of the new rail the wheel presented higher von-Mises stress for the rail cant of zero and lower stress for the cant of 1/40. For the zero cant, 1/40 and 1/20 the following results in von-Mises stress were obtained at a maximum depth of 947 MPa at 1.5 mm, 867 MPa at 3.5 mm and 867 MPa at 3.5 mm, respectively. The equal stresses for the cants of 1/20 and 1/40 is explained because the contact occurs with radiuses, both of the wheel and the rail, equal, thus respecting the Hertz equation . While the highest stress observed on the rail, in the plane, was 869 MPa for the zero cant and the lowest stress was 860 MPa, for both cants of 1/40 and 1/20, the highest stress observed along a straight line in the depth of the rail was 867 MPa to 3.75 mm depth for the zero cant and the lowest stress was 840 MPa to 3.81 mm of depth for the cant of 1/40, while the intermediate stress was 859 MPa to 3.48 mm for the cant of 1/20. However, when analyzing the location of the center of the contact ellipse it is noted that there is a significant change in its position. For the zero cant, the center of the ellipse is 12.28 mm from the centerline of the rail towards the gauge and for the cants of 1/40 and 1/20 the center of the ellipse is respectively at 6.79 mm and at 1.25 mm both also towards the gauge. When observing the equivalent conical taper for this profile for a lateral displacement of the wheelset of 10 mm, it is observed that the constant equivalent conical taper for a cant of zero, 1/40 and 1/20, respectively, up to 6.5 mm, 8.0 mm and 9.0 mm and at a value of 0.05 mm for each lateral displacement. In relation to the difference in the rolling radius, similar behavior is observed to that of the conical taper. **Error! Reference source not found.** illustrates the position of the contact points for the 3 cants for the new rail profile.

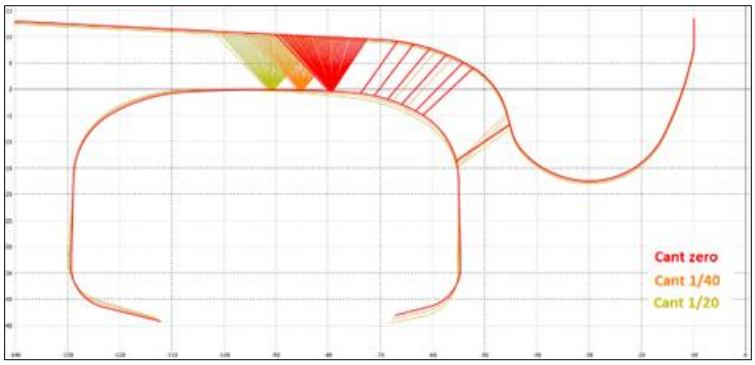

Figure 3 Contact position for the 3 cants and new rail profile

Figure 7 shows the von-Mises stresses for zero cant for the new rail profile. In this configuration, a small concentration of stresses is observed at the point where the radius of the arch of the rail of 254 mm and 31.75 mm. The curvature radiuses are highlighted in Figure 4. For this configuration the maximum stress induced by the change of curvature was 947 MPa. This fact corroborates for new rails by grinding through gradual preventive grinding to remove the least amount of material possible from the rail and smoothen the change of curvature to avoid stress concentration and consequently greater damage to the wheels and rails.

Figure 6 shows the distribution of the contact pressure on the wheel, where it is possible to see a heterogeneous distribution due to the change of radius of curvature of the rail. On the other hand, a homogeneous distribution for cants of 1/20 and 1/40 is observed, as shown in Figure 5.

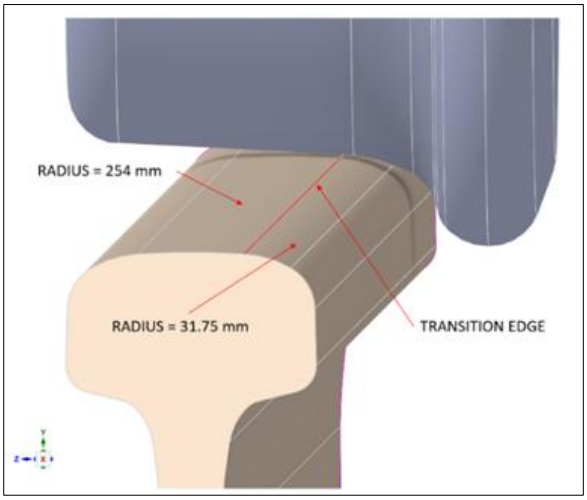

Figure 4 Illustration of the curvature transition region forming the new rail profile

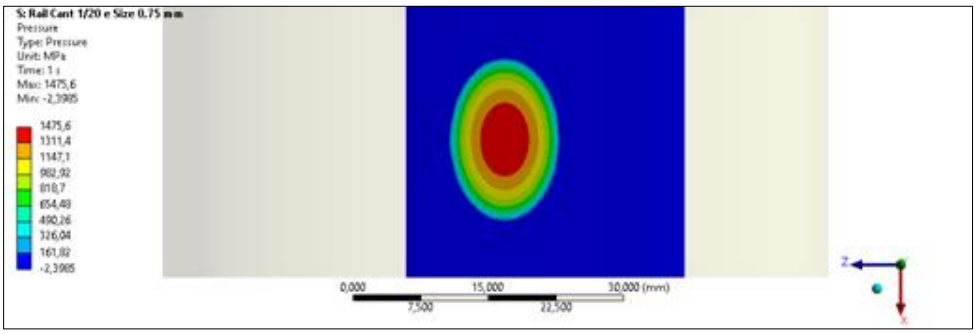

Figure 5 Contact pressure (New rail profile and cant of 1/20)

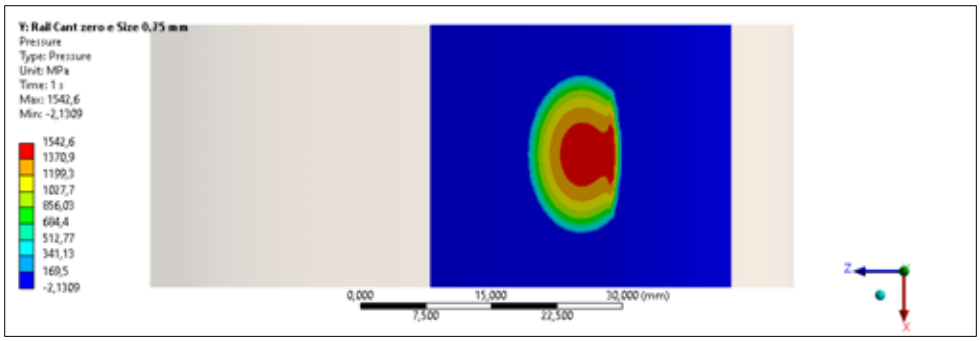

Figure 6 Contact pressure (New rail profile and zero cant)

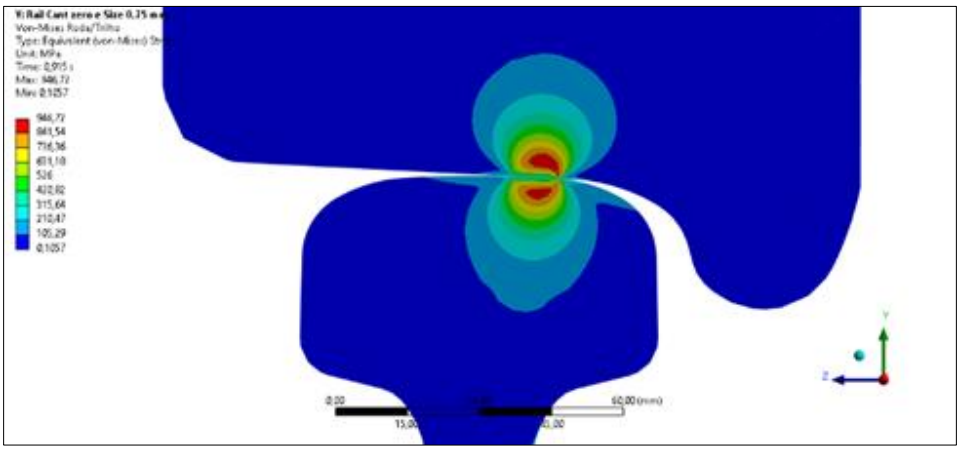

Figure 7 Von-Mises stresses (New rail profile and zero cant)

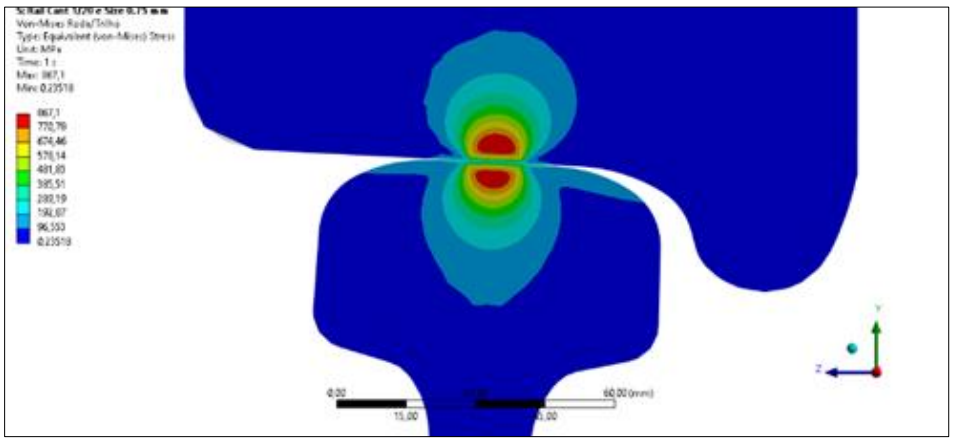

Figure 8 Von-Mises stresses (New rail profile and cant of 1/20)

The stress concentration observed for rail cant zero was not observed in the cants of 1/20 and 1/40. Figure 8 shows a homogeneous stress distribution below the surface and with von-Mises stresses of 867 MPa for the cant of 1/20 and, also, 867 MPa for the cant of 1/40.

For the three cants of the rail, plastic deformations are observed on the subsurface. With the highest value of 0.00076 mm/mm noticed in the zero cant and the lowest of 0.00036 mm/mm for the 1/40 and 1/20 cant, Figure 9 shows the plastic deformation in the pair for the zero cant. However numerically plastic deformation may seem small, there is an increase, roughly, of times, when it changes from cants of 1/20 or 1/40 to zero. This fact also reinforces the importance

of grinding for geometric re-profiling of the rail as well as serving as a warning for grinding passes that leave the side large due to the absence of grinding stones and/or an incomplete or improper grinding plan.

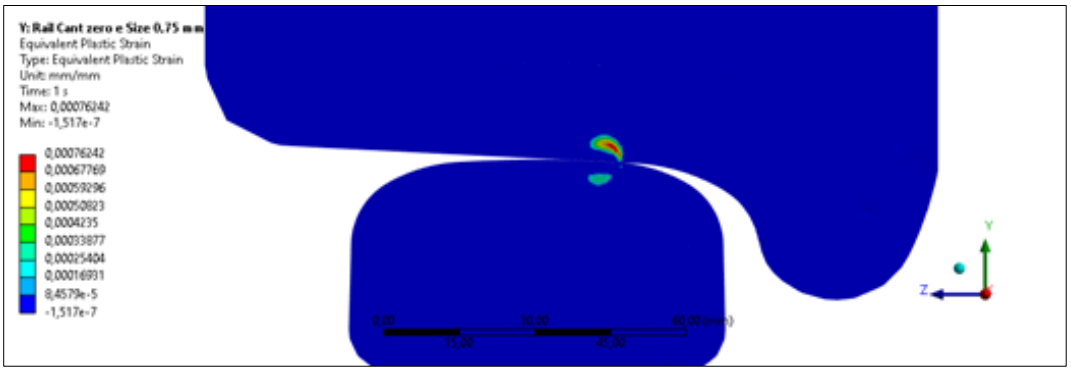

Figure 9 Plastic deformation (New rail profile and zero cant)

Figure 10 shows the voltage distribution of von-Mises for the new rail profile and in the configuration of zero cant, a configuration that shows the highest voltage with the value of 947 MPa, while the lowest voltage was 860 MPa for the cants 1/40 and 1/20.

Regarding the contact pressure, it is noted that the highest pressure was 1543 MPa for the zero cant, near the curvature transition, but in the central region of this contact the pressure was 1486 MPa. On the other hand, the maximum contact pressures for the cant of 1/40 and 1/20 were, respectively, 1474 MPa and 1476 MPa.

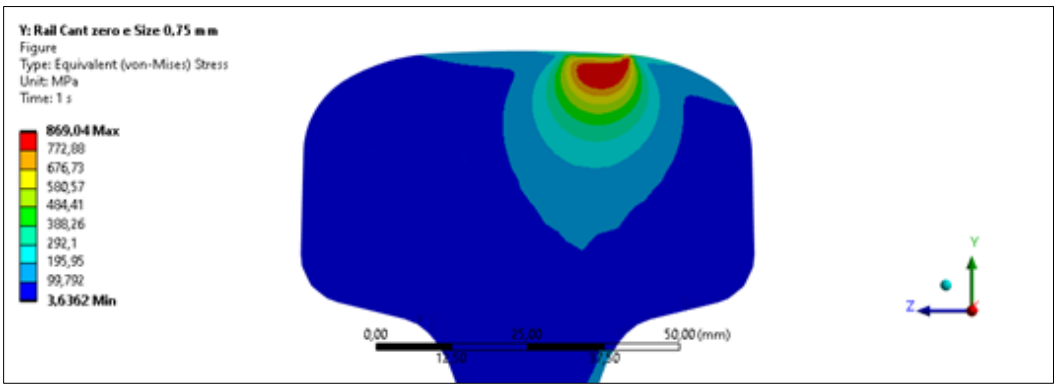

Figure 10 Von-Mises stress in the rail (New rail profile and zero cant)

As important as the location of the contact ellipse is the lateral force generated in the contact of the wheel/rail tribological pair. Considering that the higher is the lateral force, the higher is the likelihood that the rail vehicle will be unstable by some track excitation or the rolling stock, such as a track misalignment and an unbalanced load in the wagon. When talking about this excitation in a tangent, the greater the lateral force, also, the greater will be the probability of the composition generating the *hutting* effect. Figure 11 shows the reaction force on the rail. The reaction force on the wheel will have an equal module and direction and opposite direction to the reaction force on the rail. The highest lateral force observed was 16233 N for zero cant. The lowest lateral force was obtained for the 1/20 cant and its value was 12529 N. The lateral force would be intermediate for the cant of 1/40 with its value of 13551 N. In terms of L/V, the following values are given, respectively, for cant zero, 1/40 and 1/20: 0.10, 0.085 and 0.078. Comparing the results for the higher and the lower L/V value there is an increase of approximately 30% in the lateral force, that is, when the cant of the rail changes from 1/20 to zero, there is an increase of 30% of lateral force. The literature shows that force increases the wear rate of the rail significantly. Viana et al. (2020) showed that force increases in the order of 50% promote an increase in the wear rate of around 80%, according to the Archard model, in which the volumetric loss is proportional to the normal force. Thus, the 30% increase in lateral force for the 1/20 condition will promote accelerated rail wear compared to zero cant condition resulting in a longer rail life.

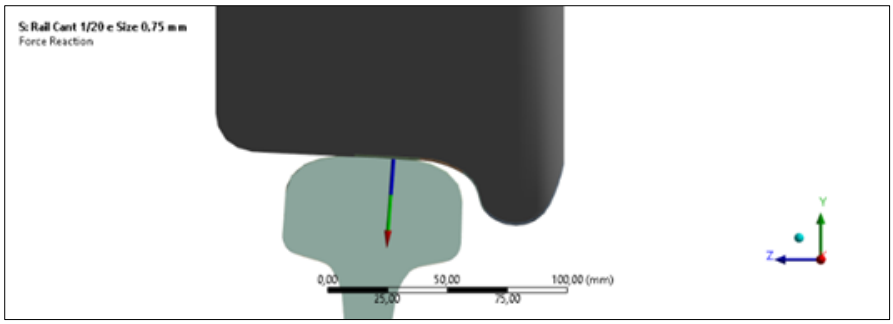

Figure 11 Reaction force in the rail (New rail profile and cant of 1/20)

It is noted that for the new rail profile when increasing the cant of the rail from zero to 1/20 the contact point moves towards the center of the rail, i.e. for zero cant the contact is closer to the gauge and for the cant of 1/20 the contact is more central. In addition, it is noted that for a lateral displacement of the 10 mm wheelset, in the conditions of cant zero and 1/40, there is contact with the flange root, according to Figure 3. Rail contact with the flange root is not observed for a 1/20 cant. The contact at the flange root should be avoided, especially in a tangent, as it can speed up wheel wear, and increase the instability of the bogie (Shevstov, 2008). The contact of the wheel flange (either at the root or on the flange itself) with the gauge corner prevailing in creeping conditions and not of rolling conditions, which leads to an increase in the wear rate of both bodies (wheel and rail), because mechanisms of wear by creeping are more severe than rolling contact fatigue mechanisms (RCF) that occur in contact between the wheel bandage and the railhead (Lewis & Olofsson, 2009; Shevtsov, 2008; Viana et al., 2020).

For the profile of the new rail, significant variations of von Mises stresses were observed as a result of the rail cant. Expressive variations of the contact position were also observed as a result of the rail cant, resulting increased lateral forces. These increases in stresses and lateral forces contribute to the increase in the rate of wear of the railway wheels, thus showing the importance of optimizing the profile of rails and the process of re-profiling via preventive or corrective grinding.

In order to reduce the damage caused, for example, in timber sleepers, the contact should be as central as possible on the rail, so that it does not generate a tipping moment on the rail and, consequently, the distribution of rail forces on the mounting plate is more homogeneous and thus, does not generate sinking towards the field gauge of the plate on the sleepers. This sinking will generate an increase decrease in gauge in addition to concentrated stresses in certain regions at the bottom of the rail foot, due to the distribution of non-homogeneous loads, which may nuclear fatigue cracks in the base of the rail foot and thus decrease railway safety, in addition to increasing maintenance costs.

For profile A, the highest von-Mises stress was 977 MPa on the wheel at a depth of 2.3 mm, for the cant of 1/40. On the other hand, the lowest observed stress was 933 MPa at a depth of 1.5 mm in the wheel for the cant of 1/20. For the cant zero, the observed stress was 953 MPa at a depth of 2.3 mm in the wheel. Shows the stresses in the von-Mises for the cants of zero and 1/20 in the contact plane. Figure 12 shows the von-Mises stress in the contact plane, it is noted that for this plane the stress was slightly higher and with the value of 981 MPa, this fact is explained by the lack of symmetry in the *Hertz* ellipse. On the other hand, the highest stresses observed on the rails were, respectively, 947 MPa at 2.68 mm of depth, 976 MPa at 2.31 mm and 931 MPa at 2.25 mm (Figure 13).

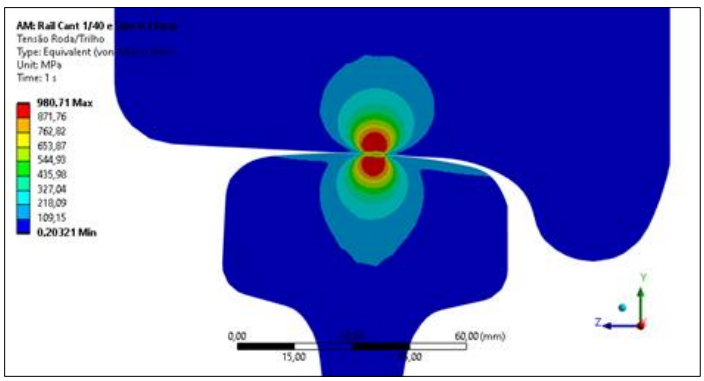

Figure 12 Von-Mises stresses (Profile A and 1/40 cant)

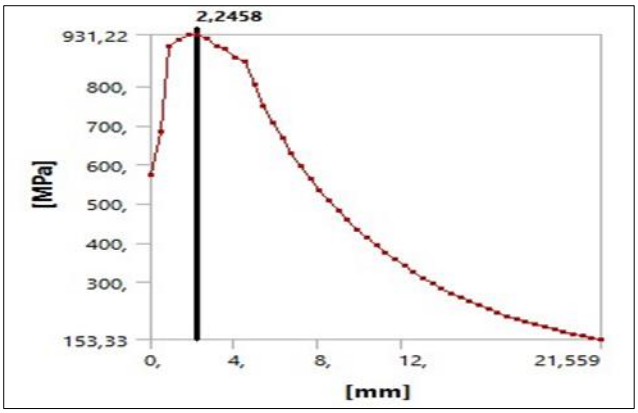

Figure 13 Von-Mises stress along a straight at the depth of the rail (Profile A and cant 1/20)

In relation to the central point of contact of the ellipse, it is noted that profile A, for all studied cants, remained the closest point to the center of the rail, with the following distances from the center of contact in the direction of the gauge of 3.47 mm, 1.99 mm and 1.01 mm for, respectively, the cants of zero, 1/40 and 1/20 (Figure 14). In addition, for all cants the flange root touched the rail for a lateral displacement of the wheelset of 10 mm.

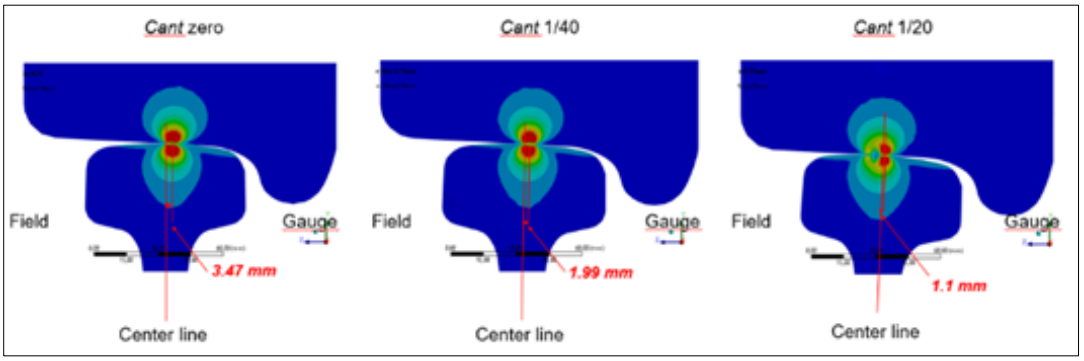

Figure 14 Contact positions for the 3 cants (Profile A)

Observing the distribution of contact pressure, higher areas with high pressures are noted, in addition to an uneven area. For the cant of 1/20 it is possible to observe two ellipses connecting to each other, as seen in Figure 15. In addition, higher contact pressures are observed than all other profiles analyzed. These contact pressures reach a maximum for the cant of 1/40 with a value of 2033 MPa and a minimum of 1882 MPa for the cant zero. The cant of 1/20 generated a contact pressure of 1964 MPa. Still in relation to the cant of 1/20, in Figure 15, due to the formation of two ellipses in the contact there will be an increase of drag forces, which will decrease the energy efficiency of the rolling stock, besides inducing greater turning moment of the bogie.

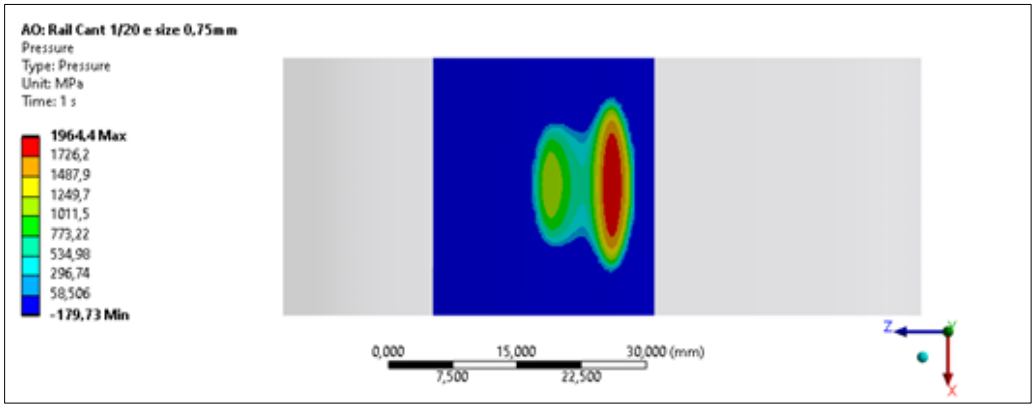

Figure 15 Contact pressure (Profile A and cant of 1/20)

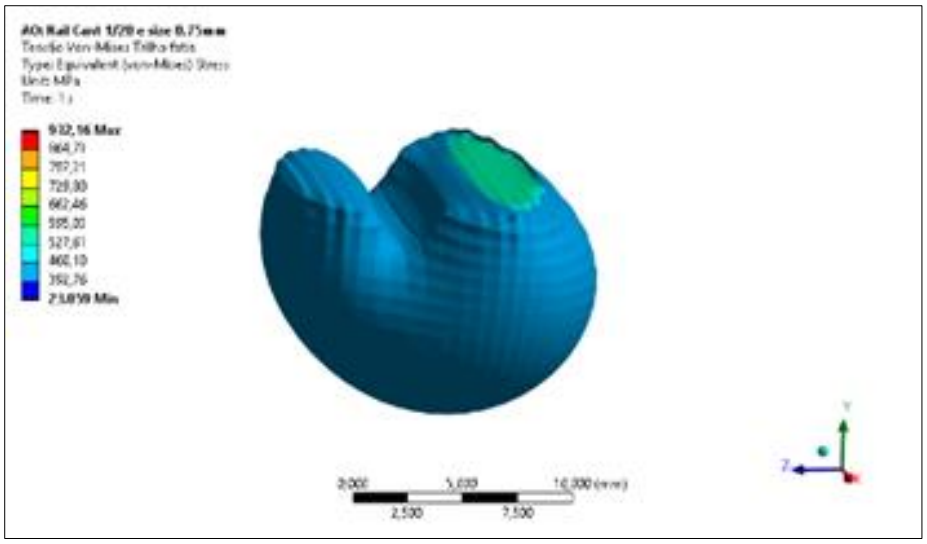

Figure 16 Von-Mises stresses in iso-surface on the rail and profile A cant of 1/20

Figure 16 shows the von-Mises stresses in the iso-surface visualization, where not only one ellipse is observed, but two joined ellipses, for profile A and cant of 1/20.

In relation to lateral force, for profile A, the highest lateral force (in module) found was 10312 N for a cant of 1/20. The lowest was 8118 N for zero cant, while the intermediate was 9670 N for a cant of 1/40. Thus, when it leaves a cant of 1/20 and goes to zero cant there is a reduction of approximately 21%. In terms of L/V there are the following values, respectively, for cant zero, 1/40 and 1/20: 0.051, 0.060 and 0.064.

In profile B, higher wheel stresses were found, of the order of 885 MPa at a depth of 3.1 mm in all cant configurations, and the lower stresses were observed in profiles C and D, having the same stresses of approximately 868 MPa at a depth of 3.5 mm, while the highest stresses found on the rails were 876 MPa at 3.1 mm of depth, 860 MPa at 3.3 mm and 860 MPa at 3.1 mm, respectively, for profiles B (Figure 15), C (Figure 17) and D (Figure 18). Regarding the contact pressures, profile B showed the highest pressure that was approximately 1560 MPa for all cants and well-defined contact ellipse with an area of around 180 mm^2. On the other hand, the pressures observed in profiles C and D were approximately 1485 MPa in all cants, in addition to a well-defined contact ellipse with an area of 187 mm^2. This fact reinforces the importance of grinding to control not only the removal of cracks and surface defects, but also to control contact stresses and pressures when there are changes in the cant.

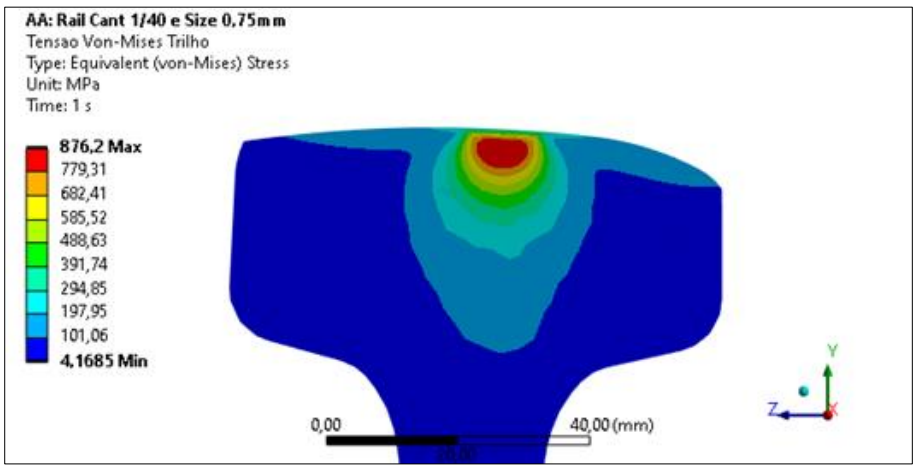

Figure 17 Von-Mises stress in the rail (Profile B and cant of 1/40)

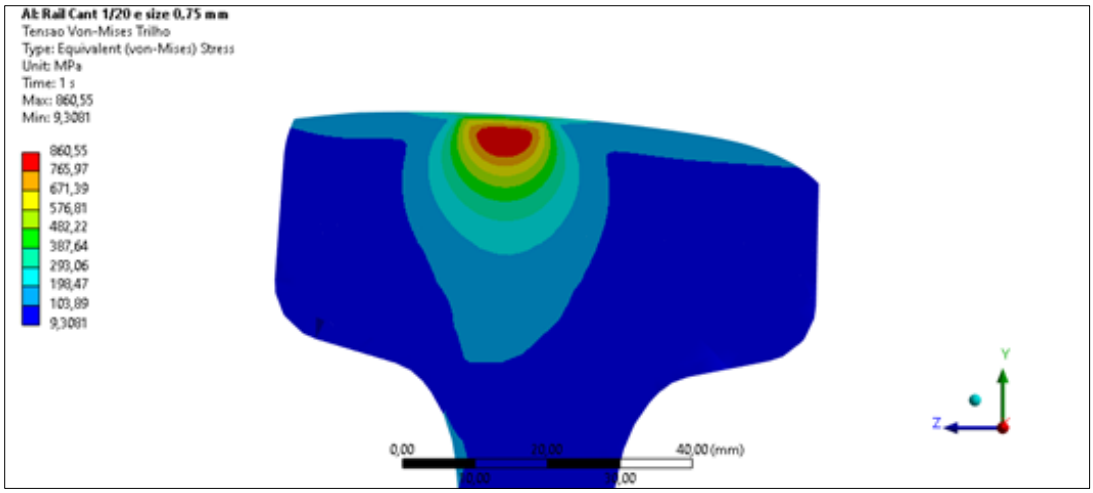

Figure 18 Von-Mises stress in the rail (Profile C and cant of 1/20)

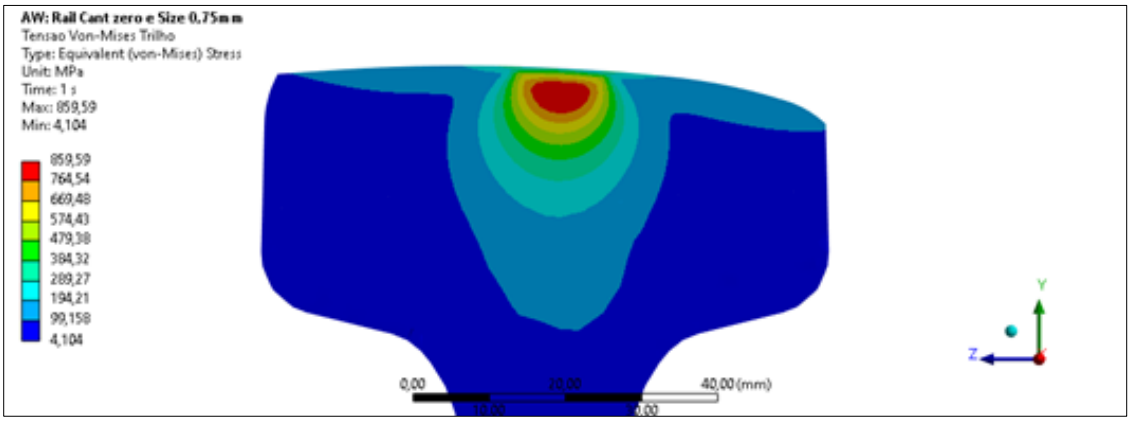

Figure 19 Von-Mises stress in the rail (Profile D and zero cant)

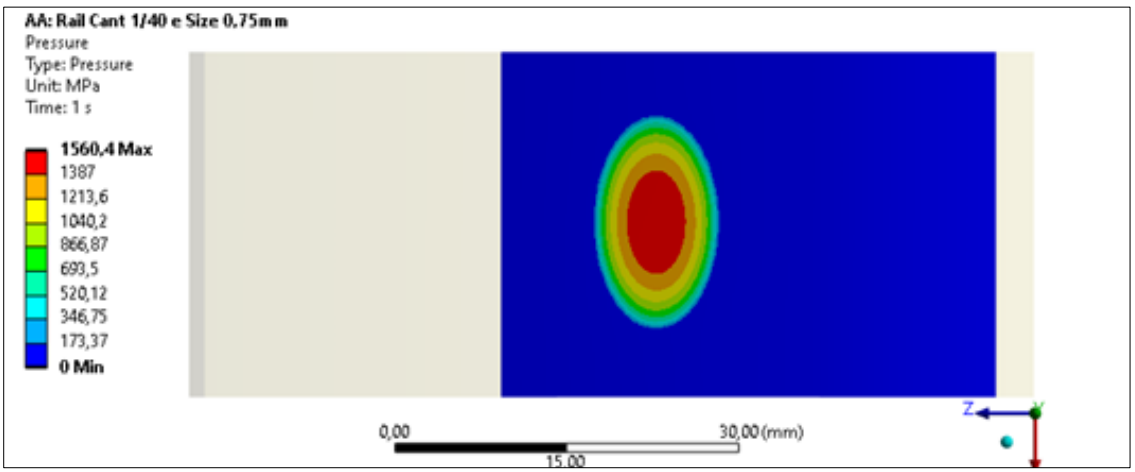

Figure 20 Contact pressure (Profile B and cant of 1/40)

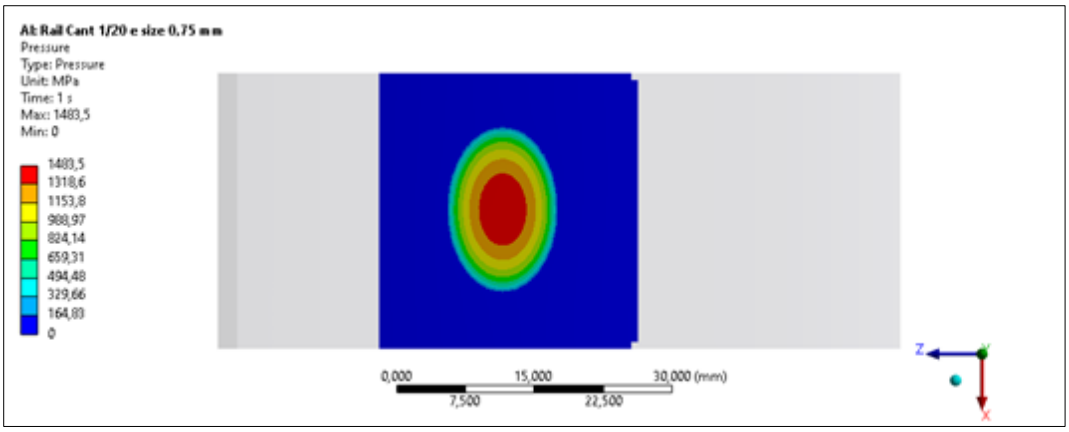

Figure 21 Contact pressure (Profile C and cant of 1/20)

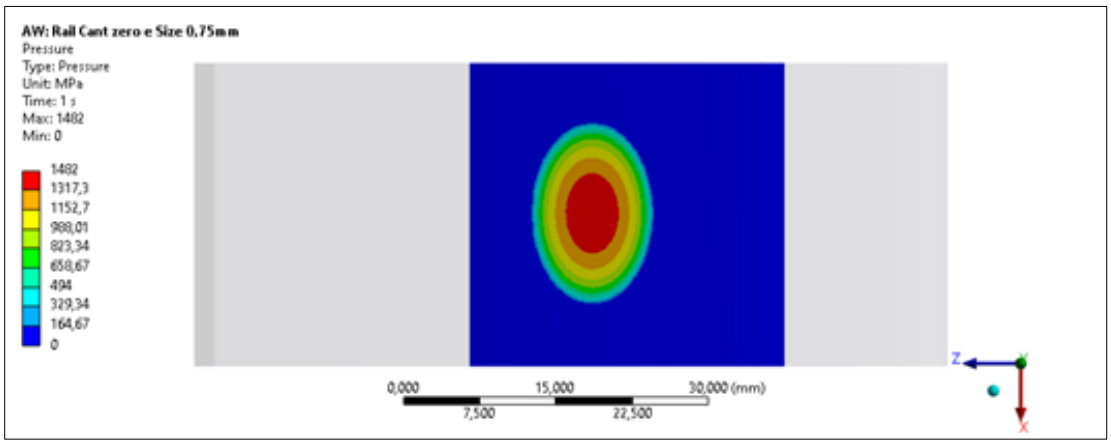

Figure 22 Contact pressure (Profile D and zero cant)

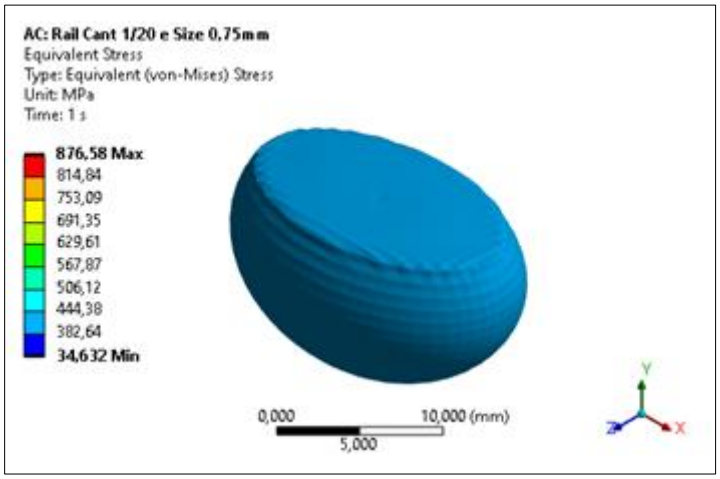

Figure 23 Von-Mises stresses in iso-surface on the rail and profile B and cant of 1/20

Figure 23 illustrates the von-Mises stresses that occur for cant 1/20 with profile B through the iso-surface. We note the formation of a single ellipse, unlike what was observed in the iso-surface for profile A (Figure 16)

Although the contact pressures and von-Mises stresses for profiles B, C and D were close, the position of the center of the ellipse varied within each profile, with the variation of the cant. Profile B had the following positions of the center of the ellipse 8.64 mm, 3.84 mm and -0.97 mm, respectively, for the cants of zero, 1/40 and 1/20. The negative signal in the position for the 1/20 cant denotes that the point is in the field direction from the center of the rail. For profile C the positions were 4.95 mm, -0.60 mm and -6.55 mm, for cants of zero, 1/40 and 1/20, respectively. Profile B had the following positions of 1.99 mm, -3.68 mm and 9.42 mm, for the cants of zero, 1/40 and 1/20, respectively.

When analyzing the behavior of the contact when moving the wheelset 10 mm laterally, it is observed in profile B that the root flange does not touch for cants of 1/40 and 1/20. However, for the zero cant the contact occurs at the flange root, as shown in Figure 24, where the green color represents the zero cant, yellow the cant of 1/40 and orange the cant of 1/20. Profile C had the same behavior as profile B when moving the wheelset 10 mm laterally. Now profile D did not have in any cant configuration and flange root contact with the rail, as shown in Figure 25.

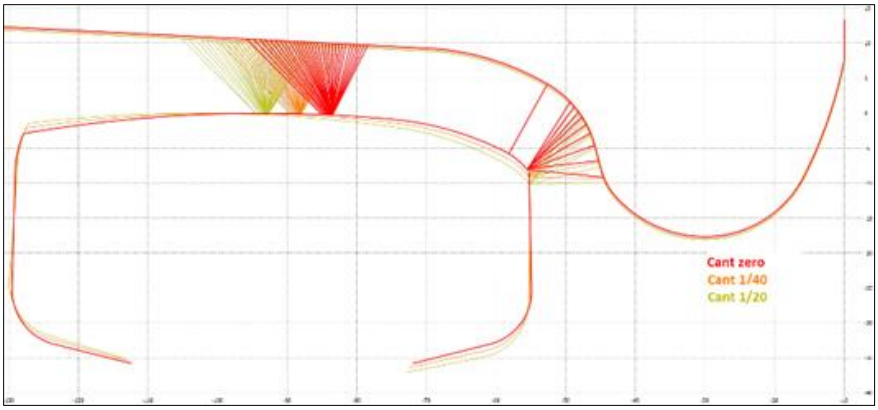

Figure 24 Contact position for the 3 cants and profile B

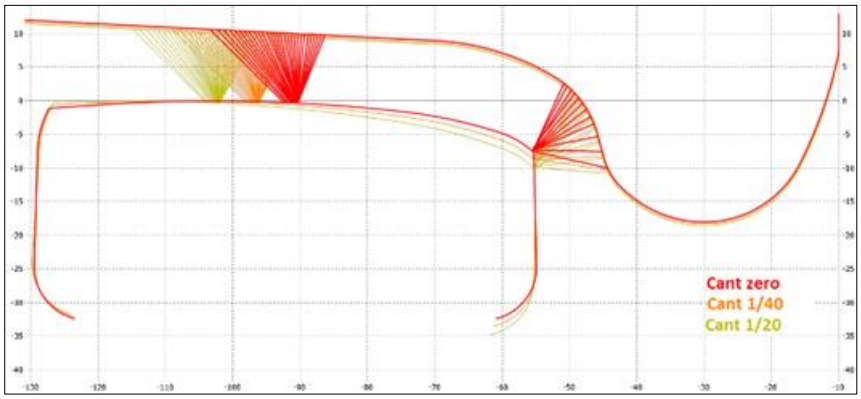

Figure 25 Contact position for the 3 cants and profile D

Regarding lateral forces, profile B had the highest lateral force (in module) found in cant zero and its value was 13562 N. The smallest was 10507 N for the cant of 1/20, which was very close to the one observed for cant 1/40, which was 10834 N. Thus, when it leaves a cant of 1/20 and goes to zero there is an increase of approximately 29%. In terms of L/V has the following values are given, respectively, for cant zero, 1/40 and 1/20: 0.085, 0.068 and 0.066. While for profile C, the highest lateral force (in module) found was 9524 N for zero cant. The lowest was 5986 N for the cant of 1/20. The intermediation was observed for cant 1/40 with the module of 7190 N. Thus, when it leaves a cant of 1/20 and goes to zero there is an increase of approximately 59%. In terms of L/V has the following values are given, respectively, for cant zero, 1/40 and 1/20: 0.060, 0.045 and 0.037. Now for profile D, the highest lateral force (in module) found was 6383 N for cant zero. The lowest was 2618 N for the cant of 1/20. The intermediation was observed for cant 1/40 with the module of 4566 N. Thus, when it leaves a cant of 1/20 and goes to zero there is an increase of approximately 143%. In terms of L/V has the following values are given, respectively, for cant zero, 1/40 and 1/20: 0.040, 0.029 and 0.016. Figure 26 shows the reaction force on the wheel with profile B and cant zero. It is observed that

the force on the wheel will have a component in -Y (vertical force) and a component +Z (lateral force). The reaction force on the rail will have the same module and the same direction, but with opposite direction to the reaction vector on the wheel.

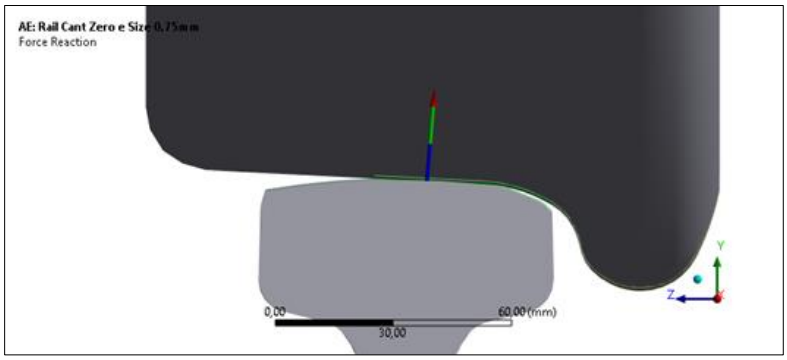

Figure 26 Reaction force on the wheel (Profile B and cant zero)

Table 1 summarizes the main results found, being possible to compare the maximum stresses and lateral forces for all profiles according to the Cant. It is noted that the lowest maximum von-Misses stress was found for the New Rail condition with a Cant of 1/40, with a value of 840 MPa. Profile A showed higher maximum value stresses, reaching 976 MPa for the Cant 1/40. The profiles: Profile B, Profile C and Profile D did not show a significant variation of the maximum stress due to the Cant and between these 3 profiles, when the Cant varied between 0 and 1/20. In summary, lower von-Mises stress values were found for the new Rail and the profiles that showed lower von-Mises stress changes due to the variation of the Cant were Profile B, Profile C and Profile D. With this result, profiles B, C and D are more suitable for conditions in which the permanent way maintenance conditions are more precarious or more time consuming, i.e., the variation of the Cant due to the degradation of track conditions will have less impact when profiles B, C and D are employed.

Table 1 Summarized results of stress, contact pressure and lateral force

		Rail			**Lateral Force (N)**
	Cant	**Maximum von-Mises Stress (MPa)**	**Maximum Stress Depth (mm)**	**Contact Pressure (MPa)**	
New Rail	0	867	3.8	1486	16235
	1/40	840	3.8	1474	13551
	1/20	859	3.5	1476	12529
Profile A	0	947	2.7	1882	8118
	1/40	976	2.3	2033	9670
	1/20	931	2.2	1964	10312
Profile B	0	876	3.1	1549	13562
	1/40	877	3.1	1560	10834
	1/20	877	3.2	1556	10507
Profile C	0	860	3.3	1458	9524
	1/40	862	3.7	1482	7190
	1/20	861	3.4	1484	5986
Profile D	0	861	3.0	1482	6383
	1/40	861	3.8	1467	4566
	1/20	862	3.1	1483	2618

As for the Lateral Force, for all conditions of Cant the New Rail presented higher values, reaching 16235 N. All profiles (A, B, C, D) obtained by grinding showed lower lateral force values, and the lowest value was for the condition with Profile D and Cant 1/40. This result highlights the importance of grinding to correct rail profiles, in order to ensure lower values of the von-Mises stress and lateral force. Considering the most general scenarios, the use of Profile D is recommended, because it presents a better combination of Maximum von-Mises Stress and lower Lateral Force values.

4. Conclusion

Significant variations of contact stresses were observed for the condition with a new rail profile, and the maximum wheel stress showed a reduction of approximately 9% when the rail cant changed from 0 to 1/40. For the other profiles, which are re-profiled, no significant variations of contact stresses were observed as a result of the rail cant.

It was observed that changing the cant from 0 to 1/20 the contact point between the wheel and the rail changes significantly. With everything, this change is more pronounced in some profiles, such as the new rail profile with a rail cant from zero to 1/20 changes the contact in the field direction by 11 mm.

When the profile does not have well-defined radius of arcs, it can cause irregular contacts by increasing the drag forces, as observed in profile B.

Regarding the lateral forces, it is concluded that when there is variation in the rail cant there are significant changes, in percentage, in the lateral forces. However, when the rail profile is ground and the arches are maintained with well-defined radiuses, there is a reduction of lateral force in all the cant configurations.

The results obtained in this study demonstrate the importance of the re-profiling performed in the preventive and/or corrective grinding process. This process is commonly used for the elimination of defects in the railheads, however, it has been shown that it also contributes significantly to the increase of the lifespan of railway wheels, by reducing contact stresses due to better contact conditions imposed by profiles more suitable than new rail profiles.

Compliance with ethical standards

Acknowledgments

The authors would like to thank Loram of Brazil for encouraging this and other studies for the development of railway solutions.

Disclosure of conflict of interest

The authors declare no conflicts of interest regarding the publication of this paper.

References

[1] Zakeri, J., Fathali, M., Roudsari, N.B. Effects of Rail Cant on Wheel-Rail Contact Forces in Slab Tracks International Journal of Mechanics and Applications 2011; 1(1): 12-21DOI: 10. 5923/j.mechanics.20110101.02

[2] Lewis, R., & Olofsson, U. (2009). Basic tribology of the wheel-rail contact.

[3] Li, W., Wang, P., Wang, S., Si, D., Yang, D. Wheel-rail wear simulation and rail cant optimisation based on railway vehicle dynamics. International Journal of Vehicle Performance, 2021, Vol. 7, No. 1-2.

[4] Ovchinnikov, D., Pokatsky, V., & Gallyamov, D. (2021). Factors Affecting the Dynamic Rail Canting of the Railway Track. Transportation Research Procedia, 54. https://doi.org/10.1016/j.trpro.2021.02.106

[5] Sadeghi, J., Fathali, M., & Boloukian, N. (2009). Development of a new track geometry assessment technique incorporating rail cant factor. Proceedings of the Institution of Mechanical Engineers, Part F: Journal of Rail and Rapid Transit, 223(3). https://doi.org/10.1243/09544097JRRT237

[6] Shevtsov, I. Y. (2008). Wheel/Rail Interface Optimisation [Delft University of Technology]. http://resolver.tudelft.nl/uuid:a728ca2a-9fa9-4b0f-959f-2fca6ca25365

[7] Viana, T. G., Tressia, G., & Sinatora, A. (2020). Sliding wear of rail and wheel steels: Effect of hardness ratio, normal load and lubrication. Tribology in Industry, 42(3), 428–442. https://doi.org/10.24874/ti.815.12.19.07

[8] Wang, P., Gao, L., Hou, B. W. (2013). Influence of rail cant on wheel-rail contact relationship and dynamic performance in curves for heavy haul railway. Applied Mechanics and Materials, 365–366. https://doi.org/10.4028/www.scientific.net/AMM.365-366.381

[9] Wang, S.; Qian, Y.U.; Feng, Q.; Luo, X.; Guo, F. Influence of rail cant on high rail side wear on sharp curve of urban transit. InVehicle-Track Interaction, Proceedings of the 2019 Joint Rail Conference, Snowbird, UT, USA, 9–12 April 2019; ASME: New York, NY,USA, 201